

Manuscript Number: CARBPOL-D-18-00415R1

Title: Thermal conductivity, structure and mechanical properties of konjac glucomannan/starch based aerogel strengthened by wheat straw

Article Type: Research Paper

Keywords: konjac glucomannan; thermal insulation aerogel; wheat straw; starch; pore size distribution; mechanical property.

Corresponding Author: Professor Fatang Jiang, PhD

Corresponding Author's Institution: Hubei University of Technology

First Author: Yixin Wang

Order of Authors: Yixin Wang; Kao Wu; Man Xiao; Saffa B Riffat; Yuehong Su; Fatang Jiang, PhD

Abstract: This study presents the preparation and property characterization of a konjac glucomannan (KGM)/starch based aerogel as a thermal insulation material. Wheat straw powders (a kind of agricultural waste) and starch are used to enhance aerogel physical properties such as mechanical strength and pore size distribution. Aerogel samples were made using environmentally friendly sol-gel and freeze drying methods. Results show that starch addition could strengthen the mechanical strength of aerogel significantly, and wheat straw addition could decrease aerogel pore size due to its special micron-cavity structure, with appropriate gelatin addition as the stabilizer. The aerogel formula was optimized to achieve lowest thermal conductivity and good thermal stability. Within the experimental range, aerogel with the optimized formula had a thermal conductivity  $0.04641 \text{ Wm}^{-1}\text{K}^{-1}$ , a compression modulus 67.5 kPa and an elasticity 0.27. The results demonstrate the high potential of KGM/starch based aerogels enhanced with wheat straw and starch for application in thermal insulation.

1 **Thermal conductivity, structure and mechanical properties of konjac**  
2 **glucomannan/**starch based** aerogel strengthened by wheat straw**

3

4 Yixin Wang<sup>1,2</sup>, Kao Wu<sup>1,2</sup>, Man Xiao<sup>1,2</sup>, Saffa B.Riffat<sup>3</sup>, Yuehong Su<sup>3\*</sup> and Fatang  
5 Jiang<sup>1,2,3\*</sup>

6 <sup>1</sup>Glyn O. Philips Hydrocolloid Research Centre at HUT, Hubei University of  
7 Technology, Wuhan 430068, China;

8

9 <sup>2</sup>School of Bioengineering and Food Science, Hubei University of Technology,  
10 Wuhan 430068, China;

11

12 <sup>3</sup>Department of Architecture and Built Environment, Faculty of Engineering,  
13 University of Nottingham, University Park, Nottingham, NG7 2RD, UK

14

15 **Abstract:**

16 This study presents the preparation and property characterization of a konjac  
17 glucomannan (KGM)/starch based aerogel as a thermal insulation material. Wheat  
18 straw powders (a kind of agricultural waste) and starch are used to enhance aerogel  
19 physical properties such as mechanical strength and pore size distribution. Aerogel  
20 samples were made using environmentally friendly sol–gel and freeze drying methods.  
21 Results show that starch addition could strengthen the mechanical strength of aerogel  
22 significantly, and wheat straw addition could decrease aerogel pore size due to its  
23 special micron-cavity structure, with appropriate gelatin addition as the stabilizer. The  
24 aerogel formula was optimized to achieve lowest thermal conductivity and good  
25 thermal stability. Within the experimental range, aerogel with the optimized formula  
26 had a thermal conductivity  $0.04641 \text{ Wm}^{-1}\text{K}^{-1}$ , a compression modulus 67.5 kPa and an  
27 elasticity 0.27. The results demonstrate the high potential of KGM/starch based  
28 aerogels enhanced with wheat straw and starch for application in thermal insulation.

29 **Keywords:** konjac glucomannan; thermal insulation aerogel; wheat straw; starch;  
30 pore size distribution; mechanical property.

31

32

33 Highlights:

34 1. Four natural raw materials were used for KGM/starch based aerogel preparation

35 2. KGM/starch based aerogel preparation via an energy efficient freeze drying  
36 method.

37 3. Starch was used to increase the mechanical strength of KGM/starch based aerogels.

38 4. Wheat straw can improve thermal insulation by affecting pore structure.

39 5. Thermal insulation mechanism of KGM/starch based aerogel was discussed.

40

41

42 **1. Introduction**

43 Although people's living standards have been greatly improved with rapid economic  
44 growth, the energy consuming level becomes much higher, raising considerable social  
45 concerns about energy crisis and environmental problems. Currently energy  
46 conservation and environmental protection have received growing attentions. To  
47 reduce CO<sub>2</sub> emissions, numbers of low-energy buildings and passive houses have  
48 been built in German (Beck, Heinemann, Reidinger, & Fricke, 2004). On the other  
49 hand, a large amount of energy is used for space heating and air conditioning,  
50 especially in extremely hot and cold climate regions, and the real estate has great  
51 potential for energy saving by rational use of resources. According to this, the  
52 European Union has set a goal for reductions in energy use and flue gas emissions  
53 (Ramírez-Villegas, Eriksson, & Olofsson, 2016). Therefore, energy conservation  
54 policy can be enforced and implemented by the development of thermal insulation  
55 materials.

56

57 Commonly, thermal insulation materials are composed of organic polymers, such as  
58 polyurethane foam, polystyrene foam, glass wool, etc. Polyurethane foam can be  
59 divided into two categories: flexible polyurethane foam and rigid polyurethane foam  
60 (Septevani, Evans, Chaleat, Martin, & Annamalai, 2015), and is often used as thermal  
61 insulation materials in the building envelop and domestic refrigerators (Janik,  
62 Sienkiewicz, & Kucinska-Lipka, 2014). However, the production of polyurethane  
63 foam relies on the unsustainable petroleum sources, as its two main components are  
64 isocyanates and polyether. Moreover, the widely use of polyurethane has produced

65 considerable amount of wastes, and these wastes usually go into landfill, which need  
66 quite long time to be degraded. Possessing extremely low density and large surface  
67 area, aerogel was invented by Kistler in 1931 (Kistler, 1931) and has also been used  
68 as insulation material, e.g. in space suit and aerospace detector (Randall, Meador, &  
69 Jana, 2011; Sabri, Marchetta, Faysal, Brock, & Roan, 2014). The heat transfer  
70 mechanism of aerogel is explained by the combination of heat conduction in solid  
71 backbone and gaseous phase and thermal radiation between the interior surfaces (Lee  
72 & Cunnington, 2012; Lu, Caps, Fricke, Alviso, & Pekala, 1995). The effective total  
73 thermal conductivity can be expressed as the solid thermal conductivity of the solid  
74 backbone, the effective thermal conductivity of the gaseous phase, and-the radiative  
75 heat exchange (Lee, Lee, Yim, Sun, & Yoo, 2002; Lu et al., 1995). Currently, most  
76 aerogel materials are prepared from inorganic or petrochemical-based feedstock, such  
77 as silica aerogels and resorcinol-formaldehyde aerogels (Mikkonen, Parikka, Ghafar,  
78 & Tenkanen, 2013). However, the degradation time of these aerogels can be quite  
79 long in nature and thus may cause harm to the environment. Therefore, alternative  
80 new, green and sustainable polysaccharide-based aerogels have attracted a lot of  
81 interests from researchers (Robitzer, Renzo, & Quignard, 2011).

82

83 As a renewable, sustainable, non-toxic material, polysaccharides including cellulose  
84 (Thakur & Voicu, 2016), hemicellulose, marine polysaccharides, starch (Miculescu et  
85 al., 2017), etc. have in common the ability to form gels in the presence of water or  
86 with other cross-linking agents (He, Sui, He, & Li, 2015), and polysaccharide

87 aerogels with different physical, thermal, optical and acoustical properties (Wang,  
88 Chen, Kuang, Jiang, & Yan, 2017) can be obtained by drying these gels through two  
89 commonly used drying methods, supercritical drying and freezing drying. Protecting  
90 structures from collapsing, the latter method, also known as lyophilization, is a  
91 low-cost and convenient method preferred by industry consisting of moving frozen  
92 water from a frozen sample by sublimation under vacuum. There have been a number  
93 of reports on the preparation of polymer materials through freeze-drying process from  
94 aqueous mixtures due to the safety and low cost (Wang, Alhassan, Yang, & Schiraldi,  
95 2013), e.g. nanocellulose aerogel (Nemoto, Saito, & Isogai, 2015), biobased poly  
96 (furfuryl alcohol) and clay aerogel (Wang, Sun, Long, Wang, & Schiraldi, 2016),  
97 alginate nanocomposite aerogels (Ke et al., 2016).

98

99 Konjac glucomannan (KGM) is an abundant, nontoxic polysaccharide found in the  
100 tuber of amorphophallus konjac plant. KGM is composed of glucose and mannose  
101 linked by  $\beta$ -1, 4 glycosidic bonds at 1:1.5–1:1.6 molar ratio, with 5–10% acetyl  
102 substitution (Davé & Mccarthy, 1997), and has high viscous property (30,000 mPa·s,  
103 1%, w/v) and high molecular weight ( $6.8 \times 10^5 \sim 9 \times 10^6$  Da) (Crosby, 2002). It can be a  
104 good skeleton material for aerogel preparation based on our previous research (Ni et  
105 al., 2016; Wang et al., 2017) . Wheat is cultivated in over 115 nations in the world,  
106 producing a huge amount of straw as a byproduct. Wheat straw is usually treated by  
107 incineration, causing serious air pollution to the environment. However, with its  
108 special cavity structure, wheat straw can be also used as thermal insulation materials

109 (Beck et al., 2004; Palumbo, Avellaneda, & Lacasta, 2015). Gelatin and starch as  
110 degradable natural materials can also be used for aerogel preparation (Chang, Chen, &  
111 Jiao, 2010; García-González, Uy, Alnaief, & Smirnova, 2012; Kenar, Eller, Felker,  
112 Jackson, & Fanta, 2014; Wang, J. et al., 2016). **Appropriate combination of different**  
113 **polymers could contribute to significant improvements on material properties**  
114 **(Corobea et al., 2016)**. According to previous research (Chen et al., 2017; Ni et al.,  
115 2016; Wang et al., 2017), the pore structure and mechanical property of KGM-based  
116 aerogels can vary a lot with different composition and formulae. Therefore, this study  
117 aims to investigate the relationship between thermal insulation property and pore  
118 structure of KGM/**starch** based aerogels enhanced with wheat straw and gelatin. The  
119 impact of aerogel components on the mechanical property, thermal stability, density,  
120 porosity of KGM/**starch** based aerogels was also studied. This research can contribute  
121 to the development of biodegradable thermal insulation materials.

122

## 123 **2. Experiments**

### 124 **2.1 Materials**

125 KGM was supplied by Licheng Biological Technology Co., Ltd. (Wuhan, China).  
126 Potato starch was purchased from Wuhan Lin He Ji Food Co., Ltd. (Wuhan, China).  
127 Gelatin was purchased from Sinopharm Chemical Reagent Co., Ltd. (Shanghai,  
128 China). Raw wheat straw was obtained from Local farmers in Wuhan. After **being** cut  
129 to small segments and washed more than 5 times, raw wheat straw was completely  
130 dried in an oven at 90 °C. The **dried straw segments** was mechanically milled into  
131 particles by a cereal pulverizer. Wheat straw powder were sieved through a 160 mesh

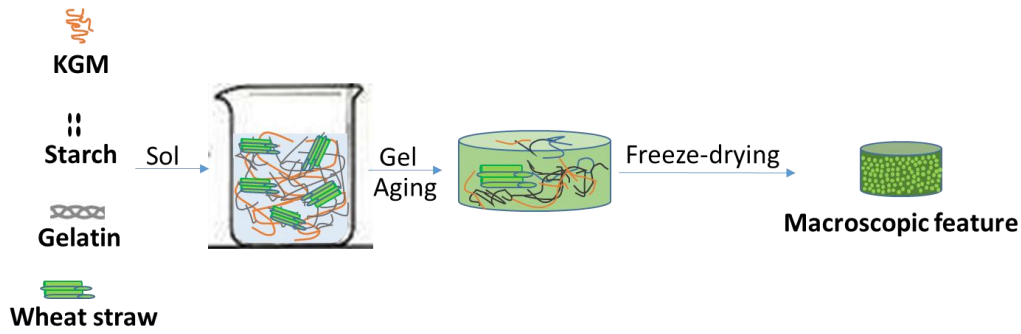


132 Tyler screen (pore size 94  $\mu\text{m}$ ) before being used.

133

## 134 **2.2 KGM/starch based aerogel preparation.**

135 The preparation of KGM/starch based aerogels was based on an invention patent of  
136 Licheng Biological Technology in China (Jiang, 2013) as illustrated in Fig. 1. Gelatin  
137 (0-1.5%, w/v) was first dissolved in double-distilled water (100 mL) in a water bath at  
138 90 °C. Then KGM (0.5-1.5%, w/v), potato starch (1.0-3.0%, w/v) and wheat straw  
139 powder (0.5-1.5%, w/v) were gradually added and mixed homogenously with the  
140 stirring speed 600 rpm for 1 h to obtain the mixed sol. Subsequently the sol was  
141 injected into a cylindrical 6 well cell culture cluster (diameter 34.8 mm and height 18  
142 mm) and put into a 4 °C refrigerator for aging and molding for 2 h, before  
143 immediately frozen in an ultra low temperature freezer (DW-FL262, Rowsen, China)  
144 at -25 °C for 10 h. The frozen sample was dried in a freeze dryer (Modulyod-230,  
145 Thermo Electron Corporation, USA) at -55 °C under a vacuum of 1 Pa for  
146 approximately 24 h, and the aerogel (34.8 mm in diameter and about 10 mm in height)  
147 was formed and obtained. All aerogel samples were coded in the form of  
148 K0S0G0WS0 (K, S, G, WS represents konjac glucomannan, potato starch, gelatin,  
149 wheat straw, respectively), and the number after K, S, G, WS indicates the weight  
150 volume percent of composition in the original sol. Prior to tests, all samples were  
151 stored in a dryer with silica gel beads and dried for 6 h at 60 °C in an oven.



152  
153 **Fig. 1. Schematic procedure of preparing KGM/starch based aerogels**

154  
155 **2.3 Characterization of KGM/starch based aerogels**

156 **2.3.1 Dry density**

157 The dry density ( $\rho$ ) was calculated by the following equation:

158 
$$\rho = \frac{m_0}{V}$$

159 Where  $m_0$  is the dry weight of aerogel,  $V$  is the volume of the aerogel samples

160 **2.3.2 Estimation of porosity**

161 Porosity is an important structure parameter of KGM/starch based aerogel, and

162 porosity of aerogels was estimated according to Shi et al. (2013). Aerogel sample was

163 weighed first ( $m_0$ ), then completely immersed in ethanol in a container and weighted

164 in total ( $m_1$ ). The container was then put in a vacuum drying oven and vacuumized

165 until no air bubble coming out of the sample. After taking out the sample from the

166 container, the container with the residual ethanol was weighed ( $m_2$ ). The porosity of

167 the sample can be calculated as below:

168 
$$\text{Porosity (\%)} = \frac{\text{Weight of ethanol in sample}}{\text{Total weight of sample and ethanol}} = \frac{m_1 - m_2 - m_0}{m_1 - m_2} \times 100\%$$

169  
170 **2.3.3 Morphology, microstructure and pore size distribution of KGM/starch**

171 **based aerogels**

172 The morphology and microstructure of KGM/starch based aerogels were observed  
173 using SEM (JSM6390LV, JEOL, Tokyo, Japan). Prior to test, aerogel samples were  
174 cut into 5 mm\*5 mm\*1 mm cubical pieces using a sharp razor blade. The cut surface  
175 of samples were coated with gold particles (Bio-Rad type SC 502, JEOL Ltd, Japan)  
176 by sputtering for 60 s, before observed at magnification of 50×, 150×, 500×, 1000×  
177 using an accelerated voltage of 30 kV. Image Pro Plus software (Media Cybernetics  
178 Inc, Maryland, America) was used to evaluate the pore size distribution of the  
179 KGM/starch based aerogels based on 6 representative SEM images.

180

#### 181 **2.3.4 Texture profile analysis**

182 The mechanical property of samples were tested by Texture analyzer (TA.XT Plus,  
183 Stable Micro Systems, Surrey, UK) equipped with a 30 kg load cell and a discoidal  
184 probe (d=100 mm, compression platen Model No. 10585) through double  
185 compression tests. The test compression rate and ratio were 60 mm/min and 30%,  
186 respectively, and the trigger force was set to 1.00 N in auto mode. The compressive  
187 strength of specimens is defined as the maximum stress during the test. Sress ( $\sigma$ ) was  
188 calculated by the following standard equations:

$$189 \quad \sigma = \frac{F}{S_0}$$

190 where  $F$  is the force (in N) applied on the sample surface,  $S_0$  in  $\text{mm}^2$ , the initial  
191 cross-sectional area of the sample.

192

#### 193 **2.3.5 Thermal conductivity measurement**

194 Thermal conductivity of samples were measured at room temperature using a Thermal

195 Conductivity Analyzer (HOT DISK TPS2500, Uppsala, Sweden). The sensor  
196 (polyimide sensor d=9.868 mm, Model No. 8563) are squeezed between two  
197 KGM/starch based aerogel specimens. The equipment was put on a stable and flat  
198 table with a heat shield. The core of the apparatus is a double spiral of thin nickel wire  
199 (Gustafsson, 1991), which acts as the heat source controlling the temperature of the  
200 sensor. An orthogonal design experiment was applied to investigate optimization of the  
201 aerogel formula to minimize thermal conductivity. 4 factors (KGM, gelatin, starch,  
202 wheat straw) and 3 levels (component concentration level) were selected according to  
203 previous results.

204

### 205 **2.3.6 Thermogravimetric analysis (TGA)**

206 TGA was carried out to determine the thermostability by weight loss in relation to  
207 temperature with a Netzsch TG 209 (Netzsch, Selb, Germany). The samples were  
208 pulverized into granules by a pulverizer. With the nitrogen flow rate 20 mL/min, the  
209 specimen was heated from 25 °C to 600 °C at heating rate 20 °C/min, and weight loss  
210 curve was recorded.

211

### 212 **2.4 Statistical analysis**

213 All tests were performed at least in triplicate. Origin Pro 8 SR4 v8.0951 (OriginLab,  
214 MA, USA) was used for figure drawing and linear regression analysis. SPSS (version  
215 19, Endicott, NY, USA) was used for Pearson correlation analysis among porosity,  
216 density, and thermal conductivity of aerogels.

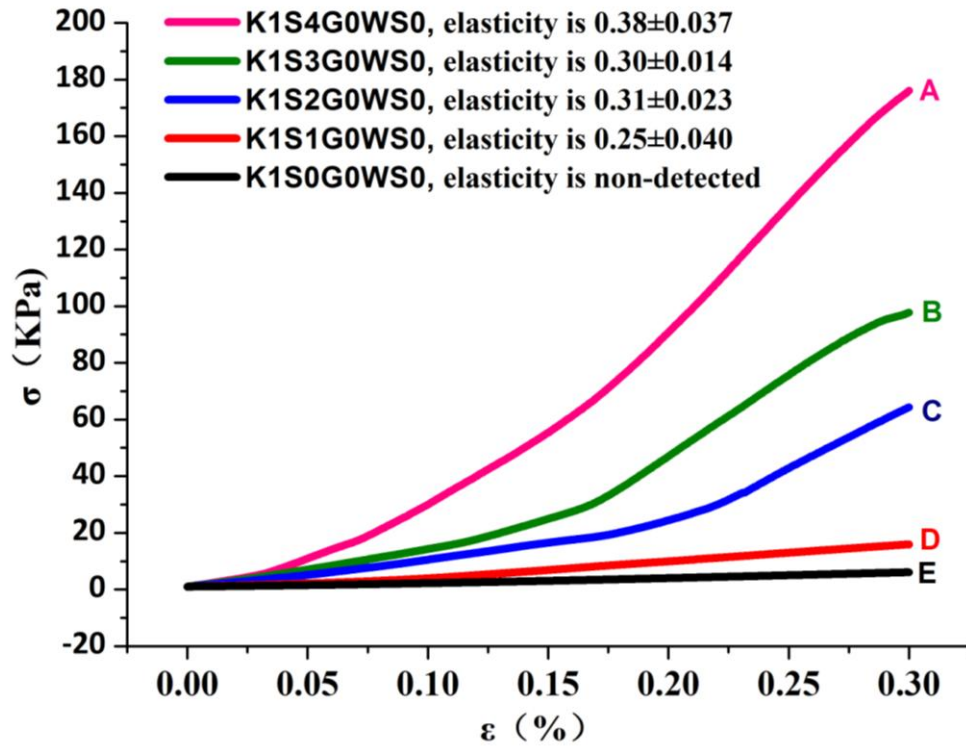
217

### 218 3. Results and discussion

#### 219 3.1 Impact of starch on mechanical property of KGM-based aerogels

220 Generally, aerogels with higher compressive stress and elasticity are suggested for  
221 practical applications. Representative stress-strain curves (strain 0-30%) for the effect  
222 of starch concentration on the compressive strength are shown in Fig. 2. The  
223 KGM-based aerogels had elasticity between 0.248 and 0.384. With starch  
224 concentration 1%, the compressive strength of aerogel was improved slightly, and  
225 starting from 2%, the compressive strength aerogel samples began to have significant  
226 increase with the increase of starch concentration. The starch addition as the filler can  
227 significantly improve the mechanical strength of the aerogels. There are two different  
228 molecular components in starch, *i.e.*, amylose and amylopectin. Amylopectin  
229 (molecular weight  $\approx 10^8$ Da) contains a significantly higher branch density than  
230 amylose (approximately 1% branch density, molecular weight  $\approx 10^4$  to  $10^6$  Da).  
231 Amylopectin is the major component in potato starch, and its branched structure could  
232 endow the structural rigidity of starch, compared with KGM molecules which are  
233 mostly linear chains without branches. Thus, starch presence could increase the  
234 mechanical properties of KGM-based aerogel samples. To be more specific, compared  
235 with K1S0G0WS0, starch addition of 1%, 2%, 3%, 4% can bring improvement of  
236 stress by 161%, 956%, 1505%, 2788%, respectively.

237



238

239 **Fig. 2. Stress-strain curves for KGM-based aerogels with different starch**  
 240 **concentration**

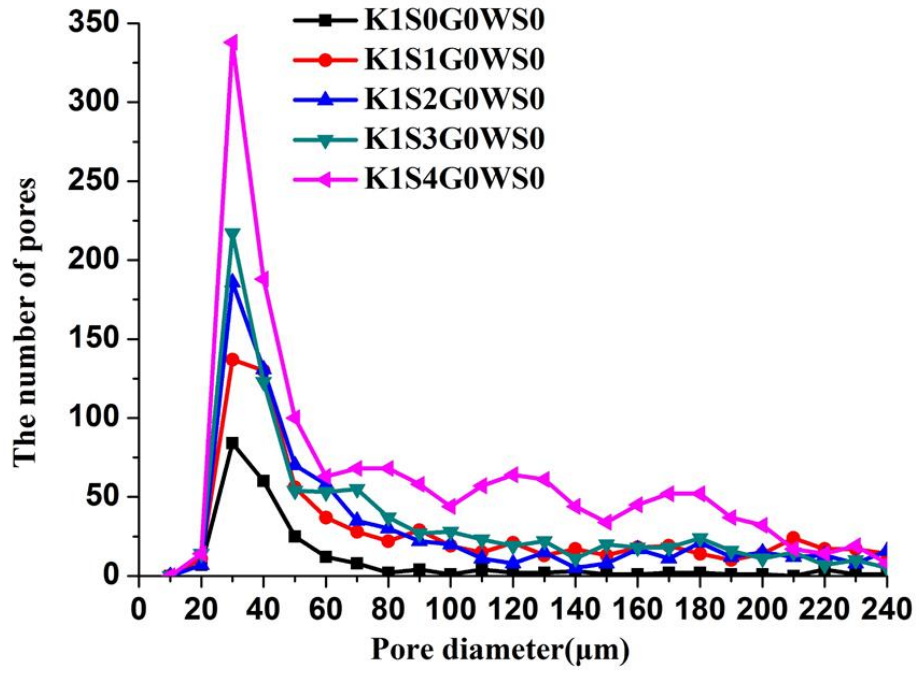
241 **3.2 Impact of starch and wheat straw on the structure of KGM-based aerogels**

242 Referring to our previous research (Ni et al., 2016), KGM-based aerogels pores are  
 243 relatively big, spherical and uniform. With starch concentration increased from 0% to  
 244 4% (w/v), the sum numbers of pores in aerogel with pore sizes 10-50  $\mu\text{m}$  were  
 245 gradually increased (Fig. 3A, B). Moreover, a good linearity ( $R^2 = 0.9240$ ) was  
 246 observed between the sum number of pores and the starch concentration (Fig. 3C).  
 247 This suggests that by varying starch concentration, the pore size of aerogels could be  
 248 adjusted to desired value through a linear model. With increased starch concentration,  
 249 the pore walls became thicker, and the pore channel size decreased. This would  
 250 benefit formation of close pores in aerogels, improving thermal insulation property  
 251 (Wang, Zhong, Wang, & Yu, 2006). However, too high starch concentration may lead  
 252 to very high density of aerogels, and this does not benefit the thermal insulation

253 capability. Therefore, starch concentration of 2% (w/v) was preliminarily selected in  
254 the following parts, as it could already significantly improve the compressive stress  
255 and pore size, compared with pure KGM aerogel (K1S0G0WS0).

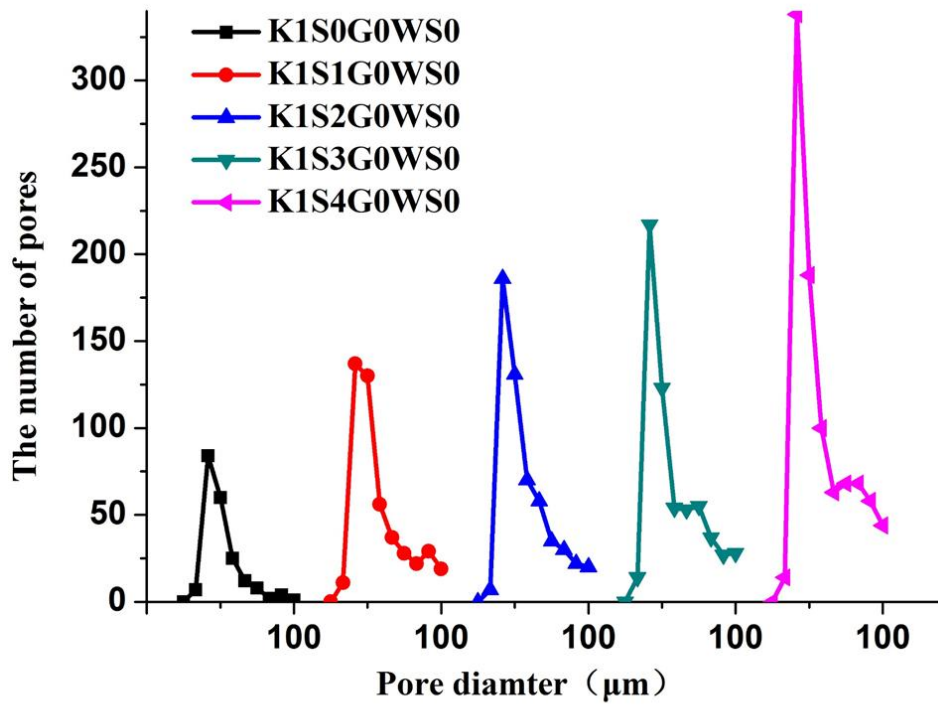
256

257 After wheat straw addition, the obtained KGM/starch based aerogels showed a  
258 greenish brown appearance with flat smooth parallel surface (Fig. 4a). Wheat straw  
259 has multi-cavities (Fig. 4b, c), and therefore with different wheat straw addition, the  
260 pore size distribution of KGM-based aerogels are adjusted, and thermal insulation  
261 properties can be changed. All KGM-based aerogels (Fig. 4d-i) had three-dimensional  
262 network structure. Without wheat straw addition, pores were almost round (Fig. 4d),  
263 and after wheat straw addition, the pores were smaller and their shapes was changed  
264 from polygons into irregular shape (Fig. 4e). This may be explained by that the wheat  
265 straw addition caused shape changes of ice crystal formed during freezing, which  
266 could affect the distribution of pore size, the shape and the connectivity of the porous  
267 network (Kiani & Sun, 2011). Besides, wheat straw can also provide many  
268 micron-scale pores due to their multi-cavities, and this was supported by the size  
269 distribution results of aerogel pores (Fig. 3D), as K1S2G0WS1.5 had much more  
270 numbers of smaller pores than K1S2G0WS0. Without wheat straw (K1S2G0WS0),  
271 the wave crest (10-50  $\mu\text{m}$ ) pores in aerogel was found to include only 48.83% of the  
272 total number (806) of pores, and when wheat straw was added, a slight spike (10-50  
273  $\mu\text{m}$ ) appeared covering 66.98% of the total number (966) of aerogel pores. Therefore,  
274 with wheat straw addition, the pore size was significantly decreased (Fig. 4).



275

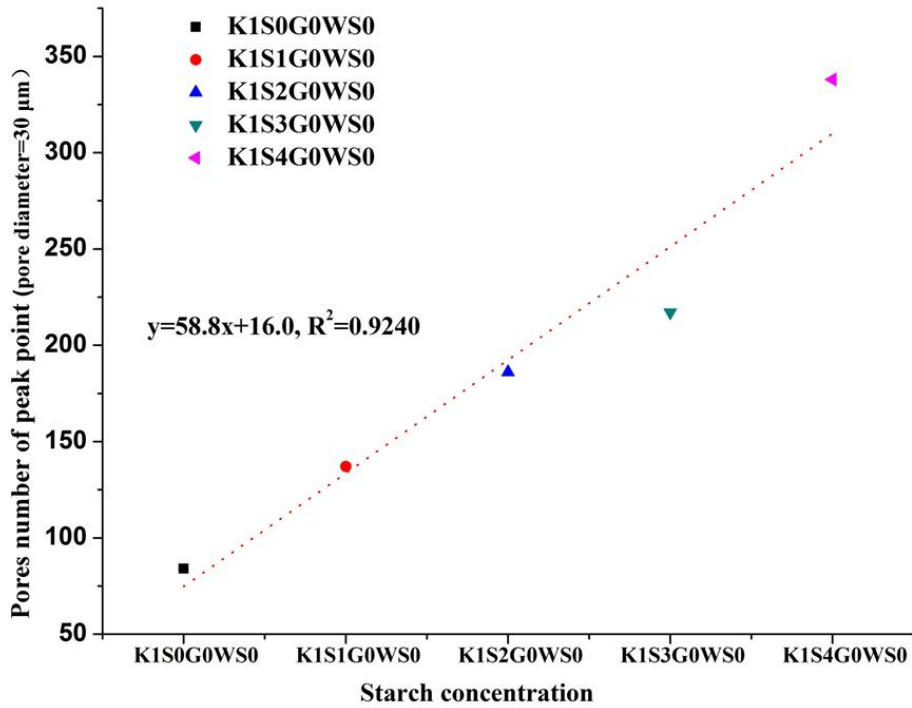
A



276

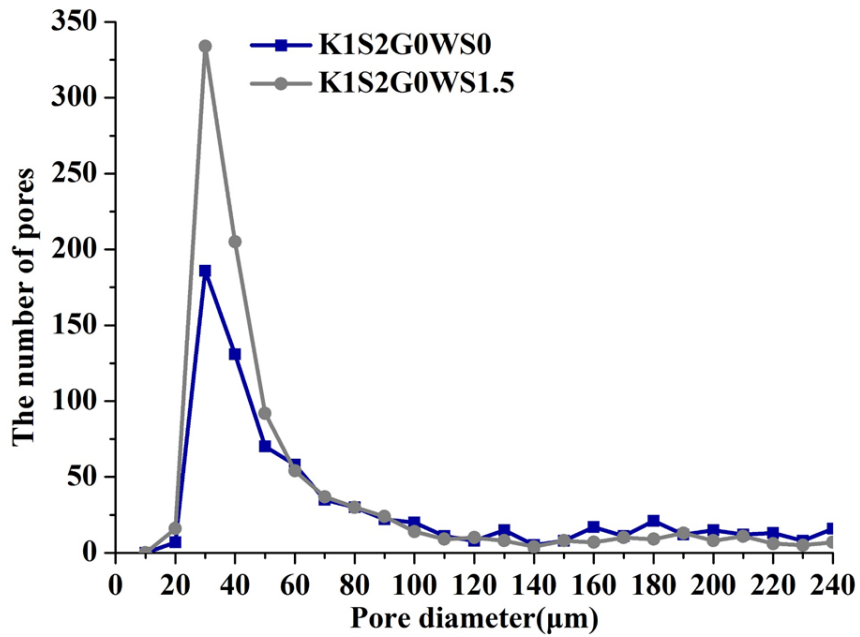
B





C

277



D

278

279

280

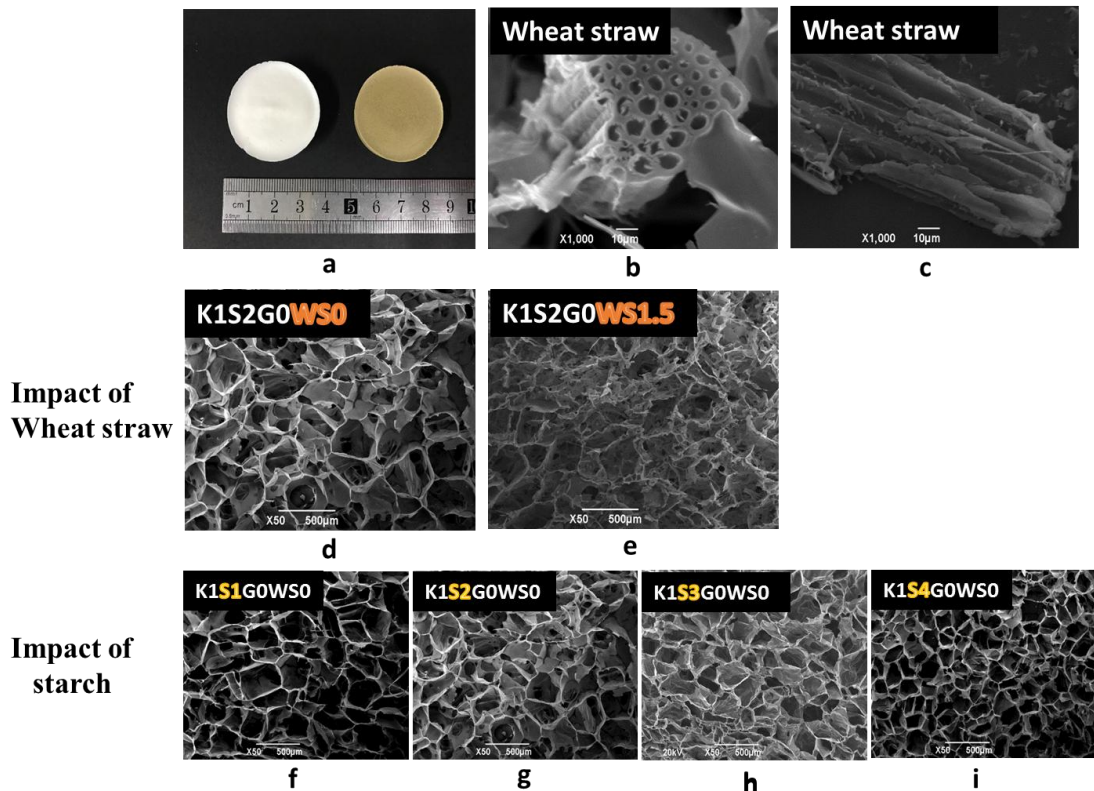
281

282

283

284

Fig. 3. (A, B) Size distribution (A: 0-240 μm; B: 0-100μm) of KGM-based aerogels pores with different starch concentration; (C) Linear relationship between starch concentration and aerogel pore numbers at pore diameter 30 μm; (D) Size distribution of KGM-based aerogels pores with different wheat straw concentration



285

286 **Fig. 4. Images of KGM-based aerogels with and without wheat straw (a), wheat**  
 287 **straw (b, c) and SEM observations of KGM-based aerogels (d-i)**

288

### 289 3.3 Thermal insulation property

#### 290 3.3.1 General heat transfer analysis for KGM/**starch** based aerogels.

291 The effective total thermal conductivity can be expressed as the sum of solid thermal

292 conductivity of the solid backbone, the effective thermal conductivity of the gaseous

293 phase, and the radiative conductivity. For KGM/**starch** based aerogel, the heat transfer

294 mechanism mainly include the solid conduction through the aerogel skeleton and the

295 gas conduction in the pores. According to this, the thermal insulation property is

296 related to the pores size distribution, pore shape, and pore walls. The solid backbone

297 of aerogels were composed of different materials whose volume heat capacity,

298 frequency-averaged mean free path of phonons and average phonons velocity are

299 invariable. However, solid conduction correlates with density which can be changed

300 by the concentration of raw materials, and the higher  $\rho$ , the higher solid heat

301 conduction  $\lambda_s$ . Low-density porous materials can have superinsulation properties as a  
302 result of the air confined in their pores when the pore size is below the free mean path  
303 of air molecules. Therefore, smaller average pore size of KGM/starch based aerogel  
304 should be preferred in order to achieve lower thermal conductivity, and this can also  
305 reduce the occurrence of open pores, which will benefit restricting gaseous heat  
306 transfer.

307

### 308 **3.3.2 Thermal conductivity of KGM/starch based aerogels**

309 Though wheat straw addition (1.5%, w/v) could improve aerogel pore size  
310 distributions, however, wheat straw subsidence occurred sometimes due to shear  
311 thinning phenomenon. As gelatin solution was found to convert into gel rapidly after  
312 the temperature was decreased to below 37 °C (Liu & Ma, 2009), it was further  
313 introduced to keep wheat straw from subsiding. We had designed a single-factor  
314 experiment to investigate the impact of gelatin on KGM-based aerogels, and the  
315 results indicated that higher gelatin addition would contribute to irregular  
316 macroscopic feature with more through-holes, which would lead to negative effect on  
317 thermal insulation (Fig. S1). However, a small number of gelatin can avoid the wheat  
318 straw from subsiding and can keep wheat straw evenly dispersive, and therefore a  
319 critical and small gelatin addition would benefit the aerogel preparation.

320

321 Based on the above results and discussion, a L9 (3<sup>4</sup>) orthogonal array test was  
322 performed to analyze the impact of different components and concentrations on the  
323 thermal conductivity and to obtain the optimized aerogel formula. Four factors (four

324 different raw materials: KGM, starch, gelatin, and wheat straw) and three levels (three  
325 different concentration) were applied, and 9 different aerogel samples were selected  
326 (Table 1). Significant thermal conductivity differences were observed among different  
327 samples. K1.0S2.0G0WS1.5 showed the lowest thermal conductivity ( $0.04683$   
328  $\text{Wm}^{-1}\text{K}^{-1}$ ), and K1.5S2.0G1.0WS0.5 had the highest ( $0.05329\text{Wm}^{-1}\text{K}^{-1}$ ). Based on the  
329 thermal conductivity values of the 9 designed samples, k and Range values were  
330 calculated and the results indicated the effect of raw material concentration on the  
331 thermal conductivity followed the order: gelatin > wheat straw > starch > KGM,  
332 according to the values of range. The optimized aerogel formula was therefore  
333 calculated to be K1S2G0.5WS1.5. To confirm this, we had prepared aerogel sample  
334 K1S2G0.5WS1.5, and its thermal conductivity was measured to be  $0.04641\text{Wm}^{-1}\text{K}^{-1}$ ,  
335 a little lower than K1S2G0WS1.5. Its compressive strength, elasticity were 80.5 kPa,  
336 0.273, respectively. This thermal insulation orthogonal test result was also in  
337 accordance with the previous discussion in mechanical property section where 2 %  
338 (w/v) starch addition was preliminarily selected. With more starch concentration, the  
339 thickness of pore walls was increased and so was the solid phase heat conduction.

340

341 Porosity, density are important factors affecting thermal conductivity. The density and  
342 porosity of all samples are shown in Table 2. Pearson correlation analysis showed that  
343 density and porosity had strong negative relationship (Pearson coefficient= -0.799,  
344  $p<0.01$ ), and both of them did not have significant relationships with thermal  
345 conductivity ( $p>0.05$ ). This was in agreement with most previous researchers who

346 found that single relationship between thermal conductivity and porosity could hardly  
347 be established, because not only the volume pore fraction but also the other factors  
348 such as pore size, shape, density and orientation can impact thermal conductivity  
349 (Francl & Kingery, 1954). In the same time, the gaseous ( $\lambda_g$ ) and the radiative ( $\lambda_r$ )  
350 conductivities reduce along with the density which relates to solid content, while the  
351 solid conductivity increase with the density (Lu et al., 1995). The thermal  
352 conductivity differences of KGM/starch based aerogels may have to be explained  
353 from the pore size and structure analysis.

354

355 From the samples listed in Table 1 and 2, we selected two aerogel samples with low  
356 thermal conductivity (K1S2G0WS1.5, K1S2G0.5WS1.5) and K1S2G0WS0 to  
357 analysis the impact of pore structure on thermal conductivity. Compared with  
358 K0.5S1G0WS0.5 which had lowest density, K1S2G0WS1.5 had smaller pores (Fig.  
359 5), leading to lower values of  $\lambda_s$  and  $\lambda_g$ . K1S2G0WS1.5 may be composed of more  
360 closed pores with main pore size distribution about 30  $\mu\text{m}$ . Compared with  
361 K1S2G0WS0, the pore wall surface of K1S2G0WS1.5 was unsmooth with some  
362 linear cavity structure which make the connectivity of the porous network more  
363 complex (Fig. 4e), due to the impact of wheat straw addition. Moreover, after adding  
364 wheat straw powder, gaseous flow path may have been changed to be more  
365 complicated leading to the lower thermal conductivity. Additionally, with many  
366 micron-scale pores, wheat straw addition could make aerogel pores (Fig. 5e, f)  
367 become more complicated which was good thermal insulation due to elongated heat

368 transfer path. Compared with K1S2G0WS1.5, the optimized formula  
 369 K1S2G0.5WS1.5 had only the differences of small amount of gelatin addition, and  
 370 this resulted in further lower thermal conductivity. This may be explained by that  
 371 wheat straw was more evenly distributed in K1S2G0.5WS1.5. Additionally, as air had  
 372 low thermal conductivity ( $0.0267 \text{ Wm}^{-1}\text{K}^{-1}$ ), the higher porosity of  
 373 K1S2G0.5WS1.5 may also contribute to its lowest thermal conductivity.

374

375 **Table 1. Analysis of  $L_9(3)^4$  test results**

Sample code	KGM	Starch	Gelatin	Wheat straw	Thermal Conductivity
	(g/100mL)				(Mean $\pm$ SD)
K0.5S1.0G0WS0.5	0.5	1.0	0	0.5	0.05147 $\pm$ 0.00050
K0.5S2.0G0.5WS1.0	0.5	2.0	0.5	1.0	0.04870 $\pm$ 0.00030
K0.5S3.0G1.0WS1.5	0.5	3.0	1.0	1.5	0.05275 $\pm$ 0.00066
K1.0S2.0G0WS1.5	1.0	2.0	0	1.5	0.04683 $\pm$ 0.00178
K1.0S3.0G0.5WS0.5	1.0	3.0	0.5	0.5	0.05166 $\pm$ 0.00012
K1.0S1.0G1.0WS1.0	1.0	1.0	1.0	1.0	0.05135 $\pm$ 0.00066
K1.5S3.0G0WS1.0	1.5	3.0	0	1.0	0.05163 $\pm$ 0.00012
K1.5S1.0G0.5WS1.5	1.5	1.0	0.5	1.5	0.04852 $\pm$ 0.00178
K1.5S2.0G1.0WS0.5	1.5	2.0	1.0	0.5	0.05329 $\pm$ 0.00017
k1	0.05098	0.05051	0.05004	0.05214	
k2	0.04995	0.04961	0.04957	0.05056	
k3	0.05114	0.05195	0.05246	0.04937	

Range	0.00120	0.00235	0.00290	0.00278
Optimal level	G>WS>S>KGM			
Major factor	1%	2%	0.5%	1.5%

**Optimized formula**

**K1S2G0.5WS1.5**

**0.04641±0.00007**

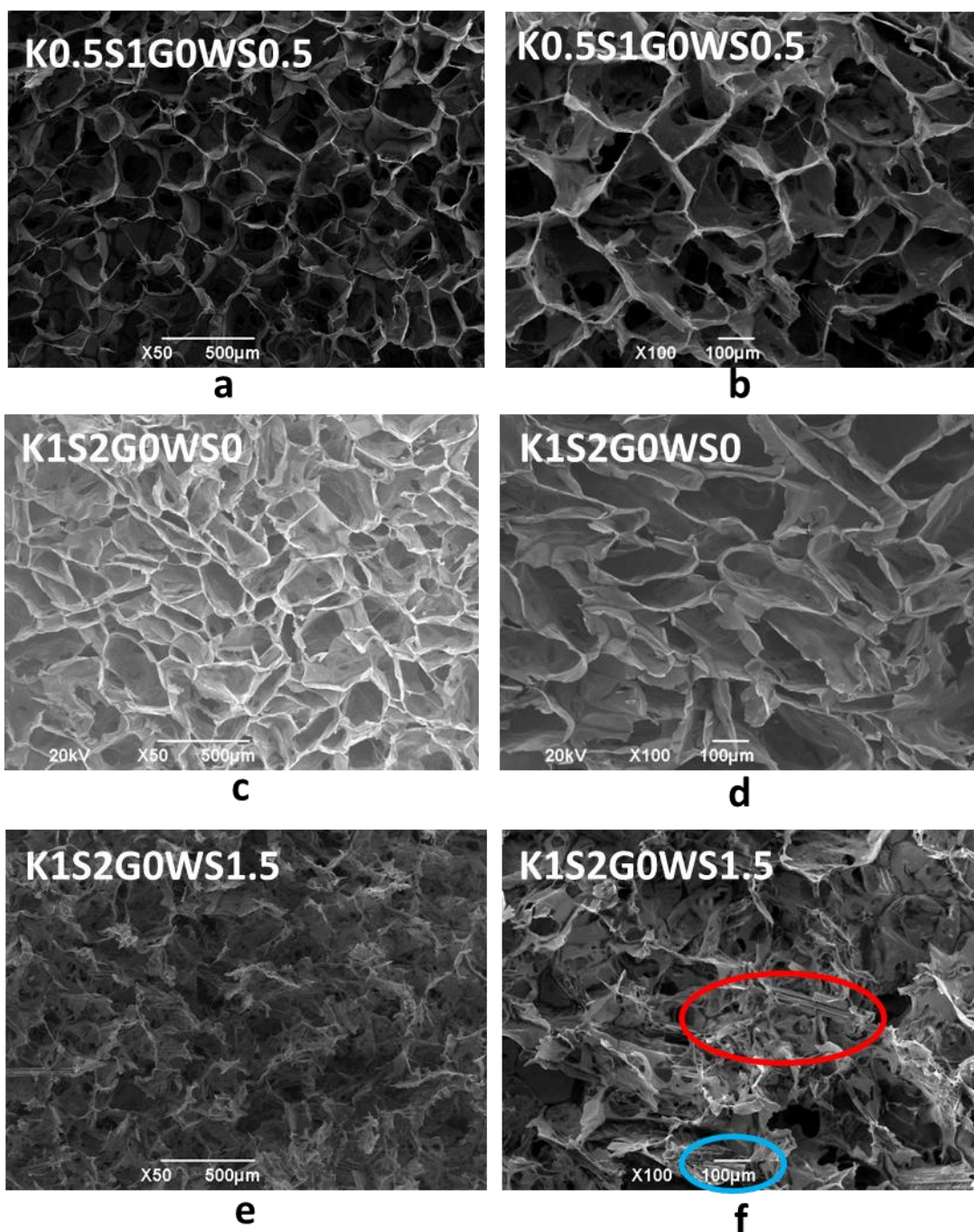
376 Range refers to the result of extreme analysis, Range = max {k1, k2, k3} – min {k1, k2, k3}. Where ki (i=1, 2,

377 3) represent the corresponding mean value of thermal conductivity at each level of concentration.

378 **Table 2. Aerogels of different composition and their porosity and density testing**  
379 **results**

Sample	Porosity (%)	Density( g/cm <sup>-3</sup> )
<b>K0.5S1.0G0WS0.5</b>	97.17±0.03	0.0201±0.0002
<b>K0.5S2.0G0.5WS1.0</b>	93.76±0.09	0.0410±0.0006
<b>K0.5S3.0G1.0WS1.5</b>	94.28±0.08	0.0524±0.0015
<b>K1.0S2.0G0WS1.5</b>	93.28±0.06	0.0409±0.0013
<b>K1.0S3.0G0.5WS0.5</b>	92.65±0.05	0.0506±0.0001
<b>K1.0S1.0G1.0WS1.0</b>	94.43±0.04	0.0358±0.0010
<b>K1.5S3.0G0WS1.0</b>	92.49±0.07	0.0471±0.0015
<b>K1.5S1.0G0.5WS1.5</b>	93.80±0.05	0.0392±0.0006
<b>K1.5S2.0G1.0WS0.5</b>	94.40±0.02	0.0437±0.0008
<b>K1S2G0.5WS1.5(Optimized formula)</b>	<b>94.50±0.03</b>	<b>0.0433±0.0002</b>

380



381

382 **Fig. 5. SEM of Samples K0.5G0S1WS0.5 and K1S2 G0WS0 and SEM**  
 383 **of Sample K1S2G0WS1.5 under different magnification 50X, 100X.**

384

### 385 3.4 Thermogravimetric analysis

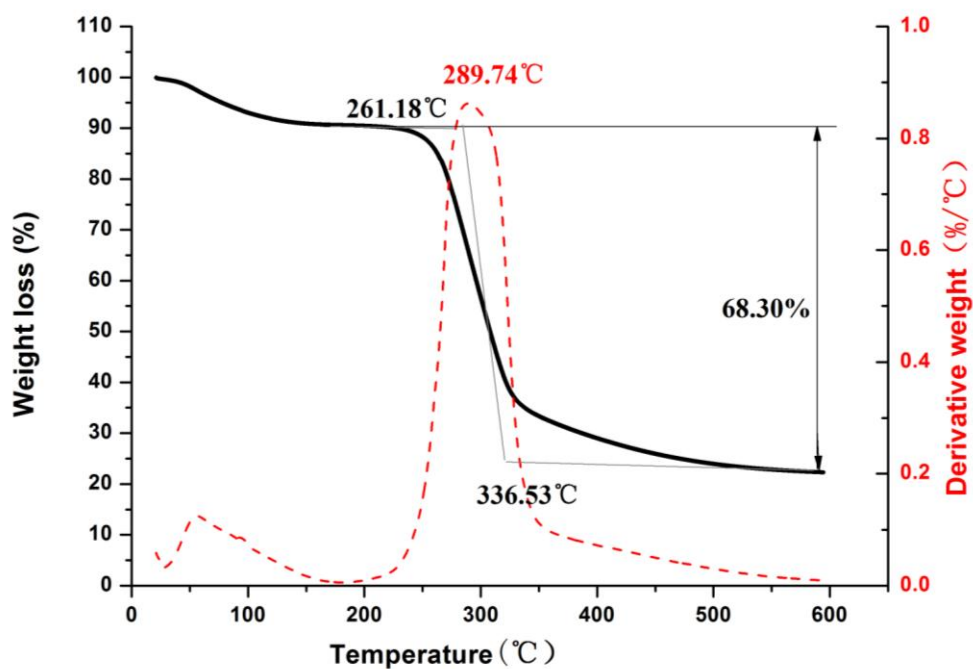
386 TG curves (**Fig. 6**) and detailed data in supplementary materials (**Table S1**) indicated

387 that KGM/starch based aerogels were decomposed in two steps. The first stage of

388 mass loss at around 100 °C in all samples corresponded to the dehydration, indicating



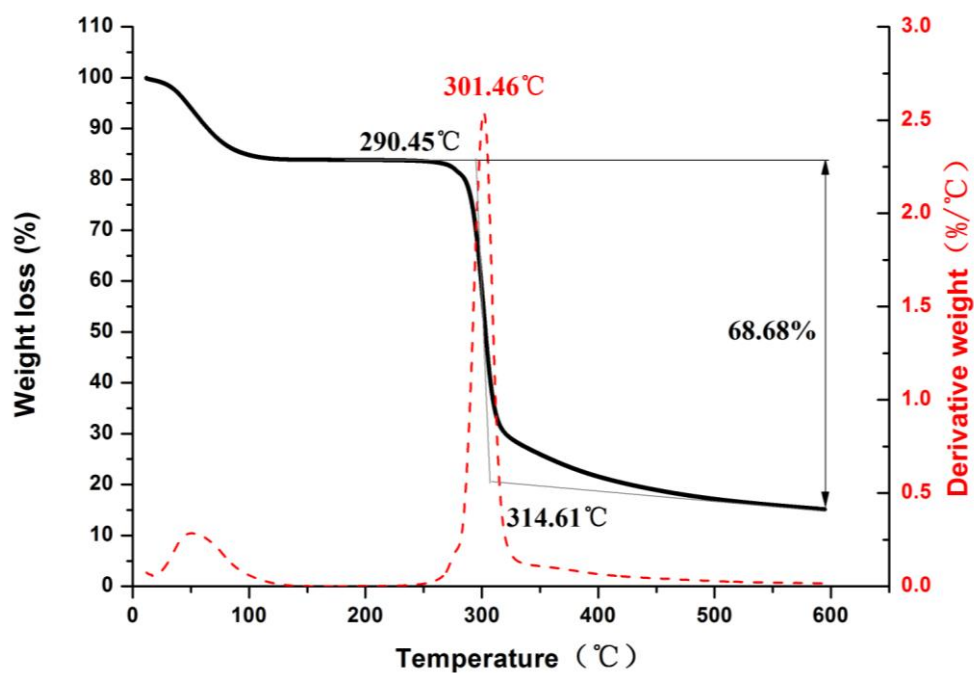
389 some moisture was still present in samples. This may be caused by the porous  
390 structure and hydrophilic nature of KGM/**starch** based aerogels, which **could adsorb**  
391 moisture from the air. The second stage of mass loss should be accredited to the  
392 pyrolysis of polysaccharide and protein, reflecting thermal stability. All sample  
393 showed similar mass loss ( $\approx 68\%$ ) during the decomposition stage. As the framework  
394 material of aerogels, KGM had a decomposition temperature from 261.18 to  
395 336.53 °C, lower than wheat straw, gelatin and starch. The mass loss stage for  
396 K1S2G0WS1.5 was from 272.62 to 344.38 °C, where around 70.90% weight was lost  
397 due to the degradation of the polysaccharide, protein and wheat straw. It can be seen  
398 that the thermal stability of KGM/**starch** based aerogel was between the properties of  
399 four pure components. At 302.98 °C, K1S2G0WS1.5 had the maximum thermal  
400 decomposition rate.



401

402

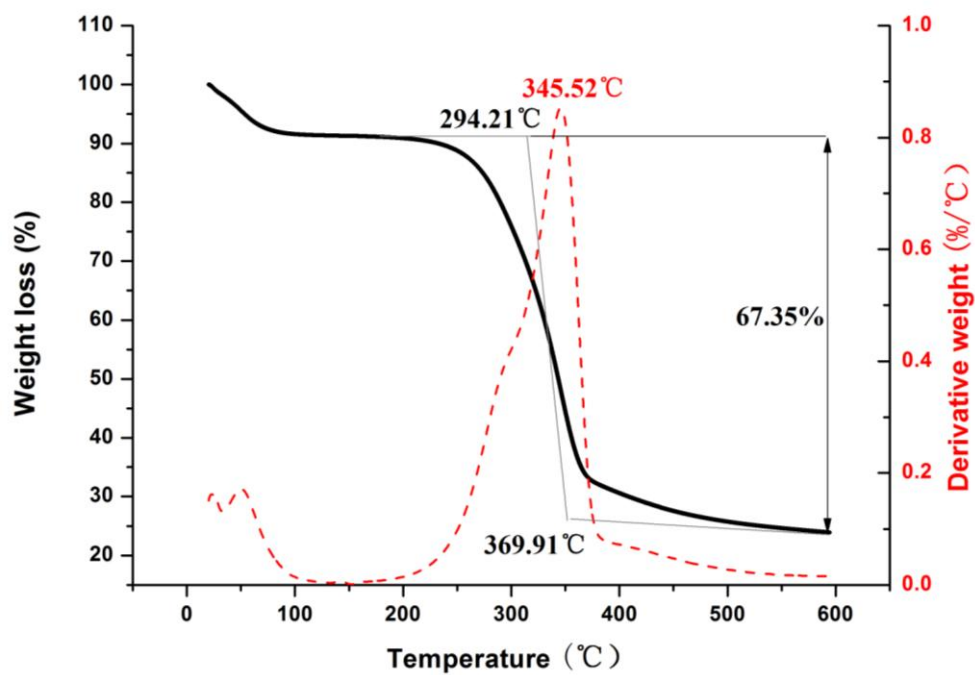
(a) KGM



403

404

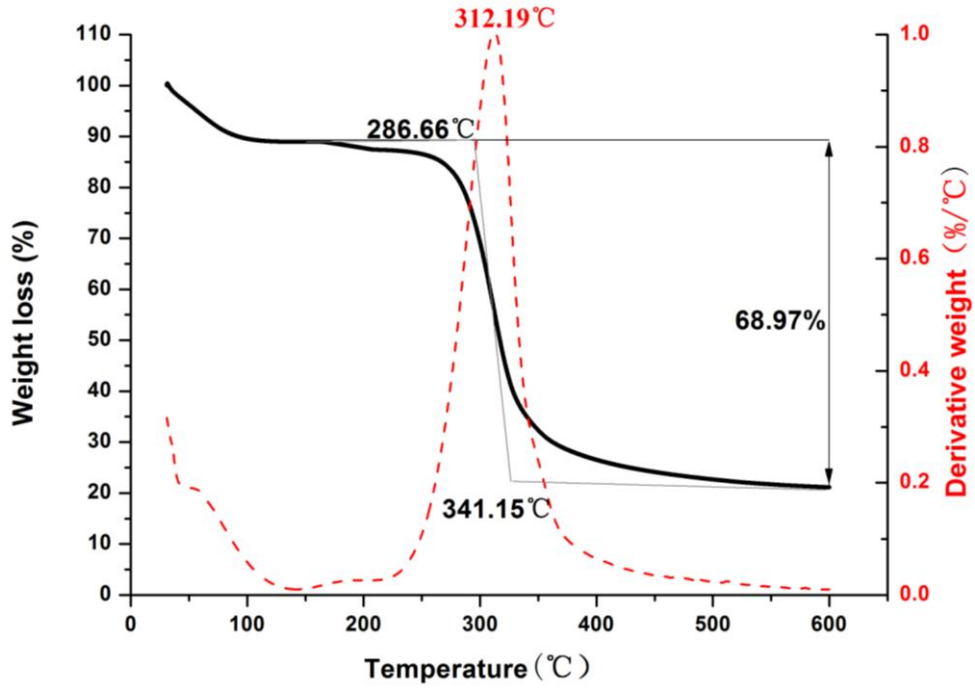
(b) Starch



405

406

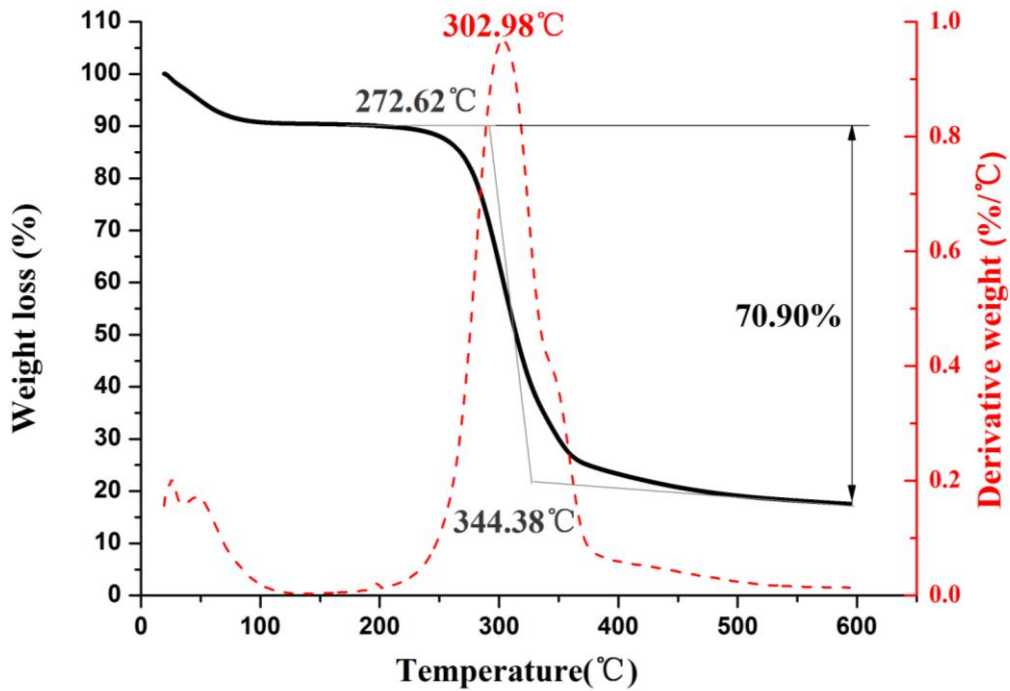
(c) Wheat straw



407

408

(d) Gelatin



409

410

(e) K1S2G0WS1.5

Fig. 6. TGA of pure raw materials and KGM/starch based aerogel

412

#### 413 4. Conclusions

414 KGM/starch based aerogels have been prepared via a convenient, energy-efficiency

415 freeze drying method. The thermal conductivity of KGM/starch based aerogels has  
416 been determined to be 0.046-0.053 Wm<sup>-1</sup>K<sup>-1</sup>. The optimized KGM/starch based  
417 aerogel sample for thermal insulation was determined to be K1S2G0.5WS2, with its  
418 thermal conductivity 0.04641Wm<sup>-1</sup>K<sup>-1</sup>, density 0.043g/cm<sup>-3</sup>, porosity 94.50±0.0291%,  
419 compressive strength 80.5kPa and elasticity 0.273. The effect of different aerogel  
420 components and their concentration on the mechanical property, porosity, density,  
421 insulation property, thermal stability, pore size distribution and structure of aerogels  
422 has been investigated. Starch can influence mechanical property, pore size, and pore  
423 wall thickness of aerogels. Wheat straw can strengthen the thermal insulation property  
424 of KGM/starch based aerogels due to the special cavity structure of wheat straw  
425 affecting aerogel pore structure and decreasing pore size. Small amount of gelatin  
426 addition is necessary to prevent wheat straw subsiding during aerogel preparation and  
427 can also improve thermal insulation property. Thermal decomposition properties of  
428 KGM/starch based aerogels fall between the values of their raw materials. This study  
429 presents a way to manufacture aerogel from natural polysaccharide materials with a  
430 satisfactory thermal insulation property.

431

432

### 433 **Acknowledgement**

434 This work is financially supported by the European Commission for the MARIE  
435 SKŁODOWSKA-CURIE individual Fellowship grant (project ID: 794680), National  
436 Natural Science Foundation of China (Grant No. 31671827) and the technology  
437 support program of Hubei Science and Technology Department (No. 2016ACA164)

438

439

440 **References**

- 441 Beck, A., Heinemann, U., Reidinger, M., & Fricke, J. (2004). Thermal transport in  
442 straw insulation. *Journal of Building Physics*, 27(27), 227-234.
- 443 Chang, X., Chen, D., & Jiao, X. (2010). Starch-derived carbon aerogels with  
444 high-performance for sorption of cationic dyes. *Polymer*, 51(16), 3801-3807.
- 445 Chen, X., Kuang, Y., Xiao, M., Wu, K., Yan, W., Jiang, F., & Huang, J. (2017). Study  
446 on adsorption of plant polysaccharide aerogels. *Science and Technology of  
447 Food Industry*, 38(11).
- 448 Corobea, M. C., Muhulet, O., Miculescu, F., Antoniac, I. V., Vuluga, Z., Florea, D., . . .  
449 Voicu, S. I. (2016). Novel nanocomposite membranes from cellulose acetate  
450 and clay - silica nanowires. *Polymers for Advanced Technologies*, 27(12),  
451 1586-1595.
- 452 Crosby, G. (2002). Managing healthy levels of blood glucose and cholesterol with  
453 konjac flour. *Special Publication- Royal Society of Chemistry*, 278, 338-341.
- 454 Davé, V., & McCarthy, S. P. (1997). Review of konjac glucomannan. *Journal of  
455 environmental polymer degradation*, 5(4), 237.
- 456 **Francl, J., & Kingery, W. D. (1954). Thermal Conductivity: IX, Experimental  
457 investigation of effect of porosity on thermal conductivity. *Journal of the  
458 American Ceramic Society*, 37(2), 99-107.**
- 459 García-González, C. A., Uy, J. J., Alnaief, M., & Smirnova, I. (2012). Preparation of  
460 tailor-made starch-based aerogel microspheres by the emulsion-gelation  
461 method. *Carbohydrate Polymers*, 88(4), 1378-1386.
- 462 Gustafsson, S. E. (1991). Transient plane source techniques for thermal conductivity  
463 and thermal diffusivity measurements of solid materials. *Review of Scientific  
464 Instruments*, 62(3), 797-804.
- 465 He, F., Sui, C., He, X., & Li, M. (2015). Facile synthesis of strong alumina-cellulose  
466 aerogels by a freeze-drying method. *Materials Letters*, 152, 9-12.
- 467 Janik, H., Sienkiewicz, M., & Kucinska-Lipka, J. (2014). 9 - Polyurethanes. In  
468 *Handbook of thermoset plastics (Third Edition)* (pp. 253-295). Boston:  
469 William Andrew Publishing
- 470 Jiang, F. (2013). Plant polysaccharide cigarette filter tip and preparation method  
471 thereof. (**Pattern NO. 102423132**). CN.
- 472 Ke, S., Wang, L., Wang, J., Wang, Y. T., Wang, Y. Z., & Schiraldi, D. A. (2016).  
473 Non-flammable alginate nanocomposite aerogels prepared by a simple freeze  
474 drying and post-crosslinking method. *ACS Applied Materials & Interfaces*,  
475 8(1), 643.
- 476 Kenar, J. A., Eller, F. J., Felker, F. C., Jackson, M. A., & Fanta, G. F. (2014). Starch  
477 aerogel beads obtained from inclusion complexes prepared from high amylose  
478 starch and sodium palmitate. *Green Chemistry*, 16(4), 1921-1930.
- 479 Kiani, H., & Sun, D. W. (2011). Water crystallization and its importance to freezing of  
480 foods: A review. *Trends in Food Science & Technology*, 22(8), 407-426.
- 481 Kistler, S. S. (1931). Coherent expanded aerogels and jellies. *Nature*, 127, 741.
- 482 Lee, O. J., Lee, K. H., Yim, T. J., Sun, Y. K., & Yoo, K. P. (2002). Determination of

483 mesopore size of aerogels from thermal conductivity measurements. *Journal*  
484 *of Non-Crystalline Solids*, 298(2–3), 287-292.

485 Lee, S., & Cunnington, G. R. (2012). Conduction and radiation heat transfer in  
486 high-porosity fiber thermal insulation. *Journal of Thermophysics & Heat*  
487 *Transfer*, 14(2), 121-136.

488 Liu, X., & Ma, P. X. (2009). Phase separation, pore structure, and properties of  
489 nanofibrous gelatin scaffolds. *Biomaterials*, 30(25), 4094.

490 Lu, X., Caps, R., Fricke, J., Alviso, C. T., & Pekala, R. W. (1995). Correlation  
491 between structure and thermal conductivity of organic aerogels. *Journal of*  
492 *Non-Crystalline Solids*, 188(3), 226-234.

493 Miculescu, F., Maidaniuc, A., Voicu, S. I., Thakur, V. K., Stan, G. E., & Ciocan, L. T.  
494 (2017). Progress in Hydroxyapatite–Starch Based Sustainable Biomaterials for  
495 Biomedical Bone Substitution Applications. *ACS Sustainable Chemistry &*  
496 *Engineering*, 5(10).

497 Mikkonen, K. S., Parikka, K., Ghafar, A., & Tenkanen, M. (2013). Prospects of  
498 polysaccharide aerogels as modern advanced food materials. *Trends in Food*  
499 *Science & Technology*, 34(2), 124-136.

500 Nemoto, J., Saito, T., & Isogai, A. (2015). Simple freeze-drying procedure for  
501 producing nanocellulose aerogel-containing, high-performance air filters. *Acs*  
502 *Applied Materials & Interfaces*, 7(35), 19809-19815.

503 Ni, X., Ke, F., Xiao, M., Wu, K., Kuang, Y., Corke, H., & Jiang, F. (2016). The control  
504 of ice crystal growth and effect on porous structure of konjac  
505 glucomannan-based aerogels. *International Journal of Biological*  
506 *Macromolecules*, 92, 1130-1135.

507 Palumbo, M., Avellaneda, J., & Lacasta, A. M. (2015). Availability of crop  
508 by-products in Spain: New raw materials for natural thermal insulation.  
509 *Resources Conservation & Recycling*, 99, 1-6.

510 Ramírez-Villegas, R., Eriksson, O., & Olofsson, T. (2016). Assessment of renovation  
511 measures for a dwelling area – Impacts on energy efficiency and building  
512 certification. *Building and Environment*, 97, 26-33.

513 Randall, J. P., Meador, M. A., & Jana, S. C. (2011). Tailoring mechanical properties of  
514 aerogels for aerospace applications. *ACS Applied Materials & Interfaces*, 3(3),  
515 613.

516 Robitzer, M., Renzo, F. D., & Quignard, F. (2011). Natural materials with high surface  
517 area. Physisorption methods for the characterization of the texture and surface  
518 of polysaccharide aerogels. *Microporous & Mesoporous Materials*, 140(1–3),  
519 9-16.

520 Sabri, F., Marchetta, J. G., Faysal, K. M. R., Brock, A., & Roan, E. (2014). Effect of  
521 aerogel aarticle concentration on mechanical behavior of impregnated RTV  
522 655 compound material for aerospace applications. *Advances in Materials*  
523 *Science & Engineering*, 2014(14).

524 Septevani, A. A., Evans, D. A. C., Chaleat, C., Martin, D. J., & Annamalai, P. K.  
525 (2015). A systematic study substituting polyether polyol with palm kernel oil  
526 based polyester polyol in rigid polyurethane foam. *Industrial Crops and*

527 *Products*, 66, 16-26.

528 Shi, J., Lu, L., Guo, W., Zhang, J., & Cao, Y. (2013). Heat insulation performance,  
529 mechanics and hydrophobic modification of cellulose–SiO<sub>2</sub> composite  
530 aerogels. *Carbohydrate Polymers*, 98(1), 282-289.

531 Thakur, V. K., & Voicu, S. I. (2016). Recent advances in cellulose and chitosan based  
532 membranes for water purification: A concise review. *Carbohydrate Polymers*,  
533 146, 148-165.

534 Wang, J., Zhao, D., Shang, K., Wang, Y. T., Ye, D. D., Kang, A. H., Wang, Y. Z.  
535 (2016). Ultrasoft gelatin aerogels for oil contaminant removal. *Journal of*  
536 *Materials Chemistry A*, 4(24).

537 Wang, T., Sun, H., Long, J., Wang, Y., & Schiraldi, D. A. (2016). Biobased  
538 poly(furfuryl alcohol)/clay aerogel composite prepared by a freeze drying  
539 process. *Acs Sustainable Chemistry & Engineering*, 4(5).

540 Wang, X., Zhong, J., Wang, Y., & Yu, M. (2006). A study of the properties of carbon  
541 foam reinforced by clay. *Carbon*, 44(8), 1560-1564.

542 Wang, Y., Alhassan, S. M., Yang, V. H., & Schiraldi, D. A. (2013).  
543 Polyether-block-amide copolymer/clay films prepared via a freeze-drying  
544 method. *Composites Part B: Engineering*, 45(1), 625-630.

545 Wang, Y., Chen, X., Kuang, Y., Jiang, F., & Yan, W. (2017). Progress in application of  
546 polysaccharide aerogels. *Journal of Wuhan Institute of Technology*, 39(5),  
547 443-449.

548 Wang, Y., Chen, X., Kuang, Y., Xiao, M., Su, Y., & Jiang, F. (2017). Microstructure  
549 and filtration performance of konjac glucomannan-based aerogels  
550 strengthened by wheat straw. *International Journal of Low-Carbon*  
551 *Technologies*.

552

553

554

555

556

557

558

559

560

**Supplementary data**

[Click here to download Supplementary data: Supplementary material.docx](#)



